Journal of Multidisciplinary Engineering Science and Technology (JMEST)
ISSN: 3159-0040
Vol. 2 Issue 7, July - 2015

Theoretical Modelling Of Thermal-Hoop Stress Around The Tooth Of A Spur Gear In A Filler Machine

[1]Salawu Enesi Yekini,[2*]Oluseyi.O Ajayi, [2]O.O Olatunji

[1]Mechanical Engineering Department, University of Lagos, Akoka, Lagos State, Nigeria
[2]Mechanical Engineering, Covenant University, P.M. B. 1023, Ota, 112101, Ogun State, Nigeria
[*]Correspondence: oluseyi.ajayi@covenantuniversity.edu.ng; +2348036208899

Abstract*—The study employed the finite element method to develop a validated theoretical model to investigate the distribution of thermal hoop stress around the teeth of a spur gear operating in a filler machine. Three cases of temperature distribution along the radius of a gear tooth were assumed and investigated. The outcome showed that *the maximum effective stress occurs at the tip of the gear tooth and decreased circumferentially deep into the gear material. The results also demonstrated that a nonlinear distribution of the temperature around the gear teeth makes the gear material susceptible to penetrating stress and therefore increase the tendency of fatigue failure.

***Keywords*—Filler machine, stress analysis, temperature variation, rotating spur gear, mechanics.**

Nomenclature

1. $\sigma_{\theta\theta}$ = hoop stress i.e. stress in the circumferential direction
2. r_2 = radius of the gear
3. $\sigma_{r\theta}$ = shear stress in θ direction
4. σ_{rz} = stress in the Z – direction
5. F_θ = local body force for unit volume
6. θ = angular coordinate
7. ρ = density of the material
8. ω = angular velocity
9. μ = Poisson ratio $0.303 \simeq$
10. E = Modulus of elasticly
11. T = Temperature (normal in ^{O}C)
12. r_i = internal radius at the root
13. r_0 = outer radius
14. σ_{cg} = stress at the tip of the tooth
15. σ_{cs} = stress at the bottom of the tooth
16. α = constant = linear expansively = 12.6 x 10^{-6}/ ^{o}C
17. β = constant
18. δ = constant
19. T_o = constant temp (minimum temperature in ^{o}C)

I. Introduction

Gear is a machine element used to transmit motion and power between rotating shafts by means of progressive engagement of projections called teeth. Generally gear transmits motion or power between rotating shafts when the centre between two shafts is comparatively low. Boddu et al [1]

The design of gears is complicated and involves the satisfaction of many constraints such as strength, pitting resistance, bending stress, scoring wear, and interference in involutes gears. This study focused on spur gear sets which are used to transmit motion between parallel shafts because of the fact that out of the various methods of power transmission, the toothed gear transmission stands unique. This is due to its high efficiency, reliability, compact layout, ability to transmit large power and simple operation. Gear designs are based on experience and engineering science. Moreover, the problem with the conventional design procedure is that it gives out a single solution and the manufacturing is carried out on that basis [2].

Critical tooth stresses affecting the reliability of spur gears are largely due to the elastic deformation of the tooth portion. Accurate assessment of these critical stresses is necessary in order to address the bending strength and thereby their load carrying capacity [3]. In some instances excessive bending fatigue stresses which exceed the material strength have led to tooth breakage and fracture conditions of the spur gear in the filler machine. This study presents an analytical evaluation of thermal hoop stress around a spur gear employed in a filler machine. This was done in order to assess the application and suitability of the analytical technique in the evaluation of the behaviour of the spur gear tooth under thermal hoop stress in a filler machine. It also focused on the investigation and evaluation of the failure rate of the gear tooth in order to reduce the filler machine's downtime.

A filler machine is a type of rotating machine which has spur gears as its main gears and usually subjected to vertical loading due to the weight of other moving components. The machine is mainly used in the bottling of brewed and distilled beverages. One major recurrent phenomenon encountered during the operation of a filler machine is the repeated failure by fatigue of the spur gear teeth. The failure causes repeated downtime and slows down production.

II. REVIEW OF PREVIOUS STUDIES

Hoop stresses are included in the advanced design and fatigue failure analysis of components in the gear transmission system, aerospace, and nuclear and automotive industries. Hoop stresses may play a

significant role in analyzing dynamic behavior of gear transmission systems. A number of studies have been performed on the dynamic behavior of gear transmission systems. For instance, Cooley and Parker [4] demonstrated unusual gyroscopic system eigenvalue behavior observed in a lumped-parameter planetary gear model. The focus was on the eigenvalue phenomena that occur at especially high speeds rather than practical planetary gear behaviour.
Handschuch and Thomas [5] developed a modeling method for analyzing the three-dimensional thermal behavior of spiral bevel gears. The study generated the model surfaces through application of differential geometry to the manufacturing process for face-milled spiral bevel gears. Contact on the gear surface was found by combining tooth contact analysis with three-dimensional Hertzian theory. The tooth contact analysis provides the principal curvatures and orientations of the two surfaces. This information was then used directly in the Hertzian analysis to find the contact size and maximum pressure during meshing which is determined as a function of the applied load, sliding velocity, and coefficient of friction. A nonlinear finite element program was used to conduct the heat transfer analysis. This program permitted the time- and position-varying boundary conditions, found in operation, to be applied to a one-tooth model.
Ebrahim [6] did a work on fault detection in gear train system which is important in order to transmit power effectively. The study discovered that vibration signals extracted from rotating parts can be used for the condition monitoring of the operating machine. Further processing of these raw vibration signatures measured at a convenient location of the machine unravels the condition of the component or assembly under study. The study also investigated the faults that occur in the spur gear and compared fault signs in the time and frequency domain.
Kumar et al [7] discovered that an effective gear design balances strength, durability, reliability, size, weight and cost. However unexpected gear failure may occur even with adequate gear tooth design. Failure of the engineering structures can be caused by cracks which depend on the design and operating conditions, and can be avoided by analyzing and understanding the manner it originates [8-9]. Moreover, various studies have investigated and predicted crack propagation paths for a variety of gear tooth geometry at various crack initiation locations and the effects of gear tooth thickness, pitch radius, and tooth pressure angle have been considered. Such analyses have been carried out using Finite Element Method (FEM) with the principles of linear elastic fracture mechanics and mixed mode fracture criteria. The stress intensity factors are the key parameters to estimate the characteristics of a crack.
In addition to the aforementioned, Raghu et al [8] did a study on the characteristics of spur gear system including the contact analysis stress, bending stress and transmission error of the gear with design and mesh. It investigated spur gear transmission error and found that it arose because of irregular shape, tool geometry, imperfect mounting and misalignment of two gears among others. The effect of the tooth profile geometry and their modification using FEM was also studied. The teeth deflection was calculated using the bending, shear and principal stresses. Jungang et al [9] also used FEM to simulate the residual stress field of planetary gear. The study employed the thermal compression stress generated by the temperature difference to simulate the gear's residual stress and therefore established the Finite Element (FE) model of the planetary gear train. The dynamic meshing process was also simulated and the influence of residual stress on equivalent stress of addendum, pitch circle and dedendum of internal and external meshing planetary gear tooth profile were analyzed. It concluded that the equivalent stresses of planetary gear at both meshing and non-meshing surfaces were significantly and differently reduced by residual stress.
Based on aforementioned, it has been found that a good number of research carried out on spur gears generalised their analyses without restricting the analysis to the areas where gears are applied. Therefore an analytical method was employed to model the behaviour of a spur gear under thermal hoop stress effects in a rotating filler machine and to determine the point of highest stress effect on the gear tooth. The very purpose of the research was to theoretically investigate and possibly provide explanation on the very reason behind the repeated failure experienced in using spur gears in rotating filler machines.

III. Procedures for Model Development and Analysis

Many engineering components are solids of revolution about an axis of geometric symmetry. Therefore, a convenient coordinate system is needed to describe such a component. This study made use of cylindrical polar coordinate system. The angular direction about the axis and the axial direction are respectively shown in Figs. 1 and 2. The hoop stress is the stress along the circumference of the gear tooth.
Based on the focus of the study, consideration was given to a simple spur gear in a rotating filler machine of specification 40 x 40 x 10 as manufactured and assembled by its maker. This machine brand was subjected to procedures that mimic the operation and then an analytical method was employed for the model development and the result obtained were characterized to establish the dynamic effects of thermal stress variation around the tooth of the spur gear. Three cases were considered for the analysis. The cases involved a hypothetical constant temperature, and the real situations of linear and nonlinear variations of temperature along the radius of the tooth.

A. Gear material and properties

The gear material was mild steel and the following properties of mild steel were employed for the analysis.
E=Young Modulus of elasticity = 210000 MPa.

$\boldsymbol{\rho}$ = density obtained as 7850 kg/m^3
$\boldsymbol{\alpha}$= $linear\ expansivity\ of\ mild\ steel\ given\ as\ 12.6 \times 10^{-6}/^0C$
$\boldsymbol{\upsilon}$ = Poisson ratio of mild steel given as 0.303 approximately.

B. Modelling procedure

The modelling procedure consists of a set of governing equations, which were derived from stress equilibrium equations and solved analytically using the polar coordinate system. The final equations were obtained based on the following assumptions:

1. 1-dimensional stress in the hoop direction and
2. 1-dimensional stress in the θ-direction

CASE1: The hypothetical case of constant temperature distribution throughout the tooth of the gear i.e. $\boldsymbol{T = T_o}$
where:
T = normal temperature in degree Celsius and $\mathbf{T_o}$ = Initial temperature in degree Celsius

CASE 2: The case of linear variation of temperature with radius, represented in the form: $\boldsymbol{T = T_o + \beta r}$
where:
β = constant and **r** = radius of the gear

CASE 3: The case of non-linear variation of temperature with the radius in a form that can be represented with the equation:
$\boldsymbol{T = T_o + \beta r + \gamma r^2}$
where:
γ = constant

It is worthy of note that, the true situation of temperature distribution is expected to follow a nonlinear variation. Hence case 3 may be taken as the real situation while cases 1 and 2 can be treated as assumptions. These were used to determine the thermal effect on the gear material.

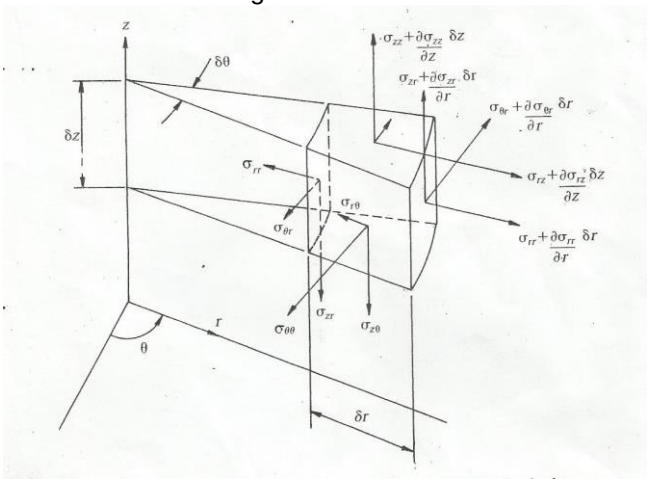

Fig. 1: Variation of stresses over a small element in a cylindrical polar coordinate system

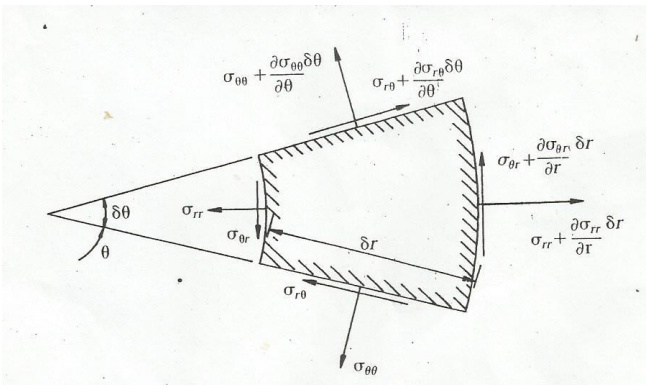

Fig. 2: Axial view of the stress variations over the element Shown in Fig. 1

Considering equilibrium in the hoop direction, the resultant hoop force on the element due to the variation of $\sigma_{\theta\theta}$ is:

$$\sigma_{\theta\theta} + \frac{\partial \sigma_{\theta\theta}}{\partial \theta}\delta\theta(\theta + \delta\theta)\delta r\delta z - \sigma_{\theta\theta} r\delta r\delta z \qquad (1)$$

Neglecting the terms involving product of more than three coordinate increments, Equation (1) becomes:

$$r\delta\theta\delta r\delta z\left(\frac{1}{r}\frac{\partial \sigma_{\theta\theta}}{\partial \theta}\right) \qquad (2)$$

Due to hopper stresses acting on the sloping sides of the element, we have a resultant hoop force

$$-\left(2\sigma_{r\theta} + \frac{\partial \sigma_{r\theta}}{\partial \theta}\delta\theta\right)\delta r\delta z \sin\frac{\delta\theta}{2} \cong r\delta r\delta\theta\delta z\left(\frac{2\sigma_{r\theta}}{r}\right) \qquad (3)$$

$$\text{Since } \sin\frac{\delta\theta}{2} \approx \frac{\delta\theta}{2} \text{ for small value of } \frac{\delta\theta}{2}$$

As a result of shear stress variation $\sigma_{\theta r}$ in the r-direction, the hoop force is:

$$\frac{\partial \sigma_{\theta r}}{\partial r}\delta r(\delta\theta\delta z)\cos\left(\frac{\delta\theta}{2}\right) = r\delta r\delta\theta\delta z\left(\frac{1}{r}\frac{\partial \sigma_{\theta r}}{\partial r}\right) \qquad (4)$$

Similarly as a result of variation of shear stress $\sigma_{\theta z}$ in z-direction, equation (5) results

$$\frac{\partial \sigma_{\theta z}}{\partial z}\delta\theta(\delta r\delta z)\cos\left(\frac{\delta\theta}{2}\right) = r\delta r\delta\theta\delta z\left(\frac{1}{r}\frac{\partial \sigma_{\theta z}}{\partial z}\right) \qquad (5)$$

The local acceleration of the element in θ – direction is given by equation (6) as

$$\rho f_\theta \delta\theta\delta r\delta z \qquad (6)$$

If the local body force per unit volume is F_θ, and since the volume of the element is approximately;

$$r\delta r\delta\theta\delta z \qquad (7)$$

Total body force is:

$$F_\theta\, r\delta r\delta\theta\delta z \qquad (9)$$

The stress equation of small motion in the hoop forces is given by:

$$r\delta\theta\delta r\delta z\left(\frac{1}{r}\frac{\partial \sigma_{\theta\theta}}{\partial \theta}\right) + r\delta r\delta\theta\delta z\left(\frac{2\sigma_{r\theta}}{r}\right) + r\delta r\delta\theta\delta z\left(\frac{1}{r}\frac{\partial \sigma_{\theta r}}{\partial r}\right) + r\delta r\delta\theta\delta z\left(\frac{1}{r}\frac{\partial \sigma_{\theta z}}{\partial z}\right) + F_\theta\, r\delta r\delta\theta\delta z = \rho f_\theta r\delta\theta\delta r\delta z \qquad (10)$$

This gives:

$$\frac{\partial \sigma_{\theta r}}{\partial r} + \frac{1}{r}\frac{\partial \sigma_{\theta\theta}}{\partial \theta} + \frac{\partial \sigma_{\theta z}}{\partial z} + \frac{2\sigma_{r\theta}}{r} + F_\theta = \rho f_\theta \qquad (11)$$

Solving equation (11) gives:

$$\sigma_{\theta\theta} = \left[\frac{1}{r^2}\left(\frac{r_o^2 . r_i^2}{r_o^2 - r_i^2}\right)(\sigma_{cg} - \sigma_{cs}) - \left(\frac{1+3\upsilon}{8}\right)\rho\omega^2(r_o^2 - r_i^2) - E\alpha\left(\frac{1}{r_o^2} - \frac{1}{r_i^2}\right)\int rTdr\right] + \left[\left(\frac{1+3\upsilon}{8}\right)\rho\omega^2(r_i^2 - r_o^2) + \frac{r_o^2}{r_o^2 - r_i^2}(\sigma_{cg} - \sigma_{cs}) - \sigma_{cs}\right] - \left[\left(\frac{1+3\upsilon}{8}\right)\rho\omega^2 r^2 - \frac{E\alpha}{r^2}\int rTdr\right]$$

Applying the cases to model for the thermal-hoop stress

Case 1. $T = T_0$

$$\sigma_{\theta\theta} = \left[\frac{1}{r^2}\left(\frac{r_o^2 . r_i^2}{r_o^2 - r_i^2}\right)(\sigma_{cg} - \sigma_{cs}) - \left(\frac{1+3\upsilon}{8}\right)\rho\omega^2(r_o^2 - r_i^2) - E\alpha\left(\frac{1}{r_o^2} - \frac{1}{r_i^2}\right)T_o\left(\frac{r^2}{2}\right)\right] + \left[\left(\frac{1+3\upsilon}{8}\right)\rho\omega^2(r_i^2 - r_o^2) + \frac{r_o^2}{r_o^2 - r_i^2}(\sigma_{cg} - \sigma_{cs}) - \sigma_{cs}\right] - \left[\left(\frac{1+3\upsilon}{8}\right)\rho\omega^2 r^2 - \frac{E\alpha}{r^2}T_o\left(\frac{r^2}{2}\right)\right]$$

$\sigma_{\theta\theta}$ Case 2: $T = T_o + \beta r$

$$\sigma_{\theta\theta} = \left[\frac{1}{r^2}\left(\frac{r_o^2 . r_i^2}{r_o^2 - r_i^2}\right)(\sigma_{cg} - \sigma_{cs}) - \left(\frac{1+3\upsilon}{8}\right)\rho\omega^2(r_o^2 - r_i^2) - E\alpha\left(\frac{1}{r_o^2} - \frac{1}{r_i^2}\right)\left[T_o\left(\frac{r^2}{2}\right) + \beta\left(\frac{r^3}{3}\right)\right]\right] + \left[\left(\frac{1+3\upsilon}{8}\right)\rho\omega^2(r_i^2 - r_o^2) + \frac{r_o^2}{r_o^2 - r_i^2}(\sigma_{cg} - \sigma_{cs}) - \sigma_{cs}\right] - \left[\left(\frac{1+3\upsilon}{8}\right)\rho\omega^2 r^2 - \frac{E\alpha}{r^2}\left[T_o\left(\frac{r^2}{2}\right) + \beta\left(\frac{r^3}{3}\right)\right]\right]$$

$\sigma_{\theta\theta}$ Case 3: $T = T_o + \beta r + \delta r^2 = T_o\left[\frac{r^2}{2}\right] + \beta\left[\frac{r^3}{3}\right] + \delta\left[\frac{r^4}{4}\right]$

$$\sigma_{\theta\theta} = \left[\frac{1}{r^2}\left(\frac{r_o^2 . r_i^2}{r_o^2 - r_i^2}\right)(\sigma_{cg} - \sigma_{cs}) - \left(\frac{1+3\upsilon}{8}\right)\rho\omega^2(r_o^2 - r_i^2) - E\alpha\left(\frac{1}{r_o^2} - \frac{1}{r_i^2}\right)\left[T_o\left(\frac{r^2}{2}\right) + \beta\left(\frac{r^3}{3}\right) + \delta\left(\frac{r^4}{4}\right)\right]\right] + \left[\left(\frac{1+3\upsilon}{8}\right)\rho\omega^2(r_i^2 - r_o^2) + \frac{r_o^2}{r_o^2 - r_i^2}(\sigma_{cg} - \sigma_{cs}) - \sigma_{cs}\right] - \left[\left(\frac{1+3\upsilon}{8}\right)\rho\omega^2 r^2 - \frac{E\alpha}{r^2}\left[T_o\left(\frac{r^2}{2}\right) + \beta\left(\frac{r^3}{3}\right) + \delta\left(\frac{r^4}{4}\right)\right]\right]$$

The resulting equations of the cases were solved and results were generated via simulation procedures.

IV. RESULTS AND DISCUSSION

Figure 3 illustrates the plot showing how the hoop stress changes with distance along the tooth depth, as the stress effect travels from the surface into the tooth material. Further to this, Fig. 3 describes the hypothetical case where the temperature distribution is constant throughout the radius of the gear tooth.

At the point of mesh, a compressive stress is felt by the gear tooth in contact and since it is a circumferential loading (hoop stress), it is felt more at the tip where the contact is felt most. Therefore it could be observed from Fig. 3 that at the point of contact, the compressive stress is approximately 0.212 GPa. This stress decreases along the depth of the gear tooth inward in a circumferential manner until a depth of 0.2 m where it becomes constant at 0.084Ga. Beyond this depth, the tooth material experiences less stress effect.

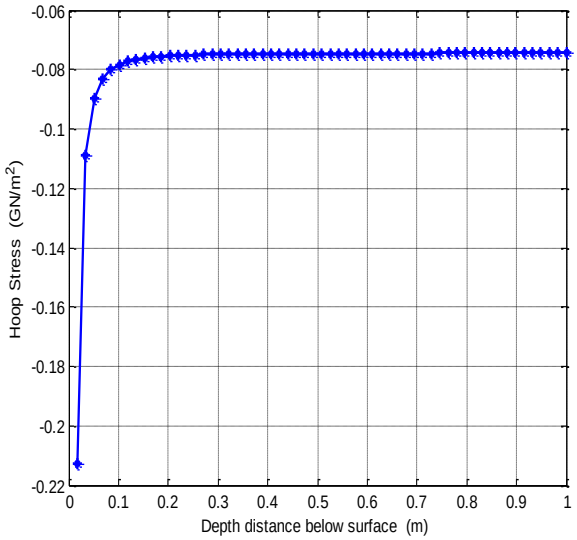

Fig. 3: Variation of hoop stress along the depth distance below surface of the tooth when the temperature is constant

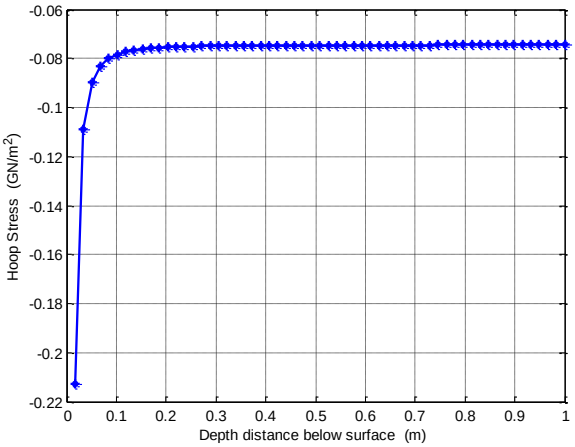

Fig. 4: Variation of hoop stress along the depth distance below surface of the tooth when the temperature varies linearly.

Figure 4 represents the case of linear variation of temperature distribution with the radius of the gear tooth. The Figure is an exact replica of Fig. 3 even though the temperature distribution varies linearly with the tooth radius. Thus, in a stress situation that leads to a linear variation described by the equation of case 2, similar results would be achieved. However the reverse is the case for a nonlinear variation of temperature distribution with radius (Fig. 5).

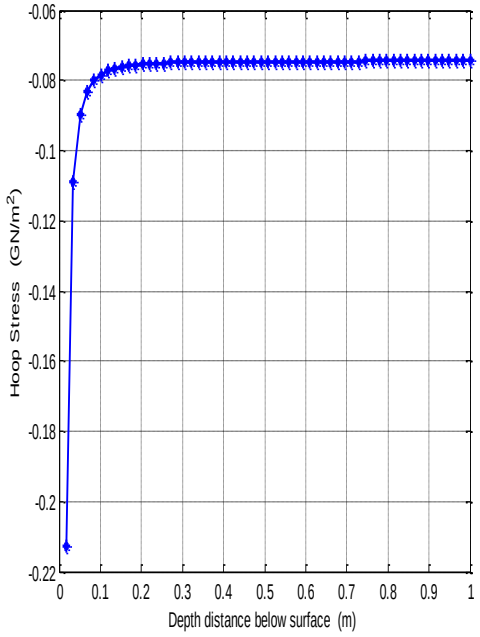

Fig. 5: Variation of hoop stress along the depth distance below surface of the tooth when the temperature varies nonlinearly.

Figure 5 shows that the effect of nonlinearity of temperature variation was felt much more along the depth. It shows that the compressive stress travels further than it did for the constant and linear variation of temperature distributions along the depth of the gear tooth. Thus while the stress effects decreases up to a depth of 0.2 m for constant and linearly varied temperatures, the stress effect for non linearity in temperature variation travelled up to the depth of 0.24 m. Hence, the nonlinearity of temperature variation makes the material susceptible to penetrating stresses. This however is the expected true practical situation of the gear in mesh while operating in a filler machine. Thus, based on this result, it can be adduced that since the teeth surfaces undergo fluctuating or cyclical compressive stresses of varying magnitudes under the action of nonlinear thermal stress distribution, fatigue failure of the material will regularly ensue. This is equally complimented by the material susceptibility to travelling stresses under the nonlinear thermal stress distribution. Moreover, in order to validate the assertion of regularity of failure, a filler machine in operation was monitored for 20 days with 12 hours of operation per day. The outcome showed that, the failure of the gear teeth was rampant with two different scenarios. The first was the non critical situation when the failures started to occur with a tooth fracture every 3 to 4 hours. As this phenomenon continued, it became critical with a tooth failure every 2 hours of operation. Slate 1 shows a pictorial view of a failed spur gear, highlighting the failed teeth.

Plate 1: Pictorial view of the failed teeth of a spur gear during an operation

V. CONCLUSION

The use of a validated analytical model to quickly and reliably assess the thermal effect of hoop stress on a spur gear strength and life has been demonstrated. This theoretical approach for hoop stress analysis was carried out for spur gear subjected to a vertical loading during operation. The analysis revealed that the maximum effective stress always occur at the tip of the gear tooth and travel down to the inside surface because of pressure at the point of contact as revealed in the non-linearity case of Fig. 5. In order to reduce the effective stress on the gear, the gear

material may be thoroughly heated both at the tip and the entire material to be able to withstand the pressure during meshing.

VI. REFERENCES

1. Boddu Anil Kumar, T.N. Charyulu "Design, Modelling and Analysis of Helical Gears" Indian streams of Research Journal, vol 2, issue 7, August 2012 pp 1-6.
2. Yallamati Murali Mohan, T. Seshaiah "Spur Gear Optimization by using Genetic Algorithm" International Journal of Engineering Research and Applications (IJERA) Vol 2, issue 1, 2012 pp 311-318.
3. Raymond J. Drago and Ravi N. Margasashayan "Stress Analysis of Planet Gears with Integral Bearings: 3D Finite element Model Development and Test Validation"
Advanced power Train Technology Group Boeing Vertol Company Philadelphia, Pennsylvania pp 1-4
4. C. G. Cooley and R.G. Parker "Unusual gyroscopic system eigenvalue behaviour in high-speed planetary gears" Journal of Sound and Vibration, vol. 332, No. 7, pp 1820-1828, 2013.
5. R.F. Handscuch and Thomas .P. Kicher "A Method for Thermal Analysis of Spiral Bevel Gears" Prepared for the International Gearing Conference ,U S Army Research Laboratory September 7-9 1994, pp 1-6.
6. Ebrahim Ebrahim "Fault diagnosis of Spur Gear using vibration analysis". Journal of American science 2012; 8(1) pp 133-138.
7. Ananda Kumar Eriki, Ravichandra R. And Mohd Edilan Mustapha"Spur Gear Crack Propagation path Analysis using FEM". Proceedings of the International mult-conference of Engineers and Computer Scientists 2012 Vol. 2 pp 978-988.
8. R. Kumar, N. Tiwaru, D. Kunwar, and R.R Vara."Transmission Error on Spur Gear" International Journal of Advanced Engineering Research and Studies. E-ISSN 2249-8974.
9. Jungang W., Yong W. and Zhipu H. "Finite Element Residual Stress Analysis of Planetary Gear Tooth" Hindawi Publishing corporation Advances in Mechanical Engineering Vol. 2013 pp 1-13